Journal of Electrical Power System Engineering & Technology
Volume 2, Issue 3, September-December, 2017

An Innovative Unique Power Converter Strategy for Distributed Generation System

Kalahasthi Rajesh Babu[1], Issarapu Reveathi[2]
Assistant professor[1, 2],
Department of EEE
VVIT, Nambur, Guntur(Dt), Andhra Pradesh, India
***Corresponding Author's email:** kalahasthirajeshbabu@gmail.com*

Abstract

Numerous advantages of a BLDC motor over a brushed DC motor in absence of the mechanical commutators which allows higher speeds. Having individual converters has advantages like more flexible individual control and simpler design but does not encourage functionality merging. As a result, power converter structure has been introduced as an alternative in high power and medium voltage situations using DG system. Distributed Generation (DG) has become increasingly more accepted since the demand for reliable and secure power systems with high power quality increases. This project presents the Distribution Generation system. The power flow is determined by controlling the amplitude and angle of displacement between the voltage produced by the DG and the grid voltage, i.e., the control variable is the same before and after the islanding mode occurs. The voltage control provides the capability to supply different kinds of loads to the DG system, such as linear, nonlinear, and motor, balanced, or unbalanced, even if the DG operates in the islanding mode. These kinds of controls are suitable for DGs operating in parallel as each of the DGs are connected to the grid through a distribution transformer (DT). Conversely, the other approaches introduced more effective. The operation of a distributed generation (DG) system driven by a dc-dc step-up converter and a dc-ac voltage source inverter (VSI) interfaced to BLDC drive *system. The simulation results are presented by using Matlab/simulink software.*

Keywords: *Distributed generation (DG), islanding modes, power converters, BLDC Drive System.*

I. INTRODUCTION

A DG based Brushless DC motors with trapezoidal Back-EMF have several inherent advantages. Most prominent among them are high efficiency and high power density due to the absence of field winding, in addition the absence of brushes leads to high reliability, low maintenance and high capability. In practice, power engineers of utilities adopt the approach, load transfer, to improve the reliability of distribution systems. Because generating facilities were not allowed to be connected to utilities' distribution systems in the past, the conventional load transfer approach is very simple for a radial distribution system. Once a fault happens in a distribution feeder, the load supplied by the faulted distribution feeder is transferred to other health distribution feeders via switching devices. The major limitation of load transfer is that the currents flowing in the health. Distribution feeders do not exceed their thermal limits.

Recently, the use of power or current in the d-q synchronous reference frame [6]–[9] as control variables to command the voltage source inverter (VSI) connected to the grid has generated considerable interest from the scientific community. With either method, before or after the contingency takes place, the control variable remains the same, making the DG operate with limited capability to supply the load. On the other hand, two control algorithms were proposed to improve the grid-connected and intentional-islanding operations methods in [10], in which the DG system must detect the situation and switch from power or current to voltage as a control variable to provide constant rms voltage to the local loads such as adjustable speed drive, in that here preferred BLDC drive as a several load demand for merely industrial applications. The main goal of this paper is grid interfaced converter strategy with closed loop control action, to regulate the voltage/current over islanding mode for

Journal of Electrical Power System Engineering & Technology
Volume 2, Issue 3, September-December, 2017

maintain constant load achievement condition. Here the dynamic analysis of proposed converter strategy is evaluated by using Matlab/Simulink platform and simulation results are conferred.

II. CHARACTERISTICS OF THE DG SYSTEM

Fig.1 shows a diagram of the system used to analyze a typical connection of a DG system to a specific feeder, although studies to determine the best site for DG insertion should be performed before the operation analysis.

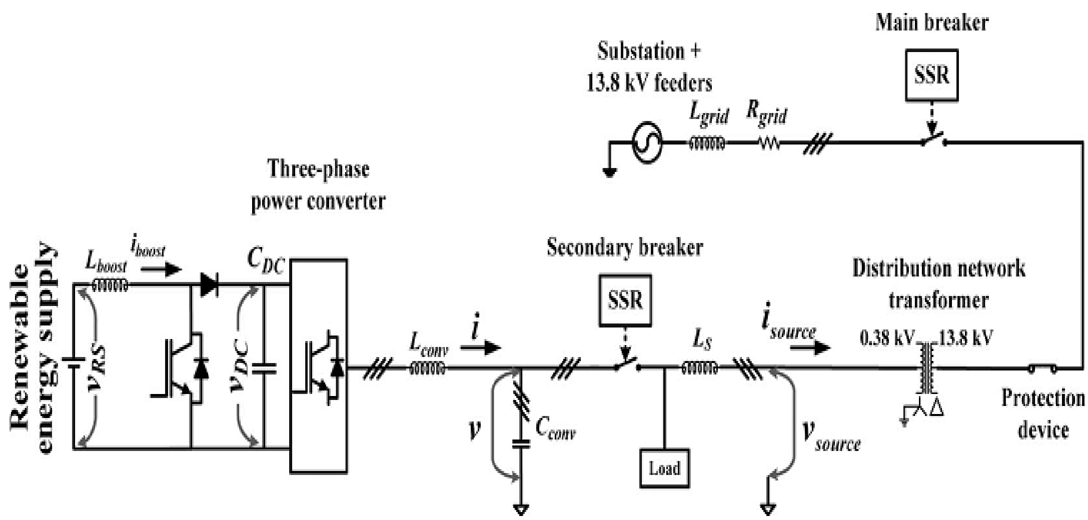

Fig.1 General Diagram of the distributed generation system

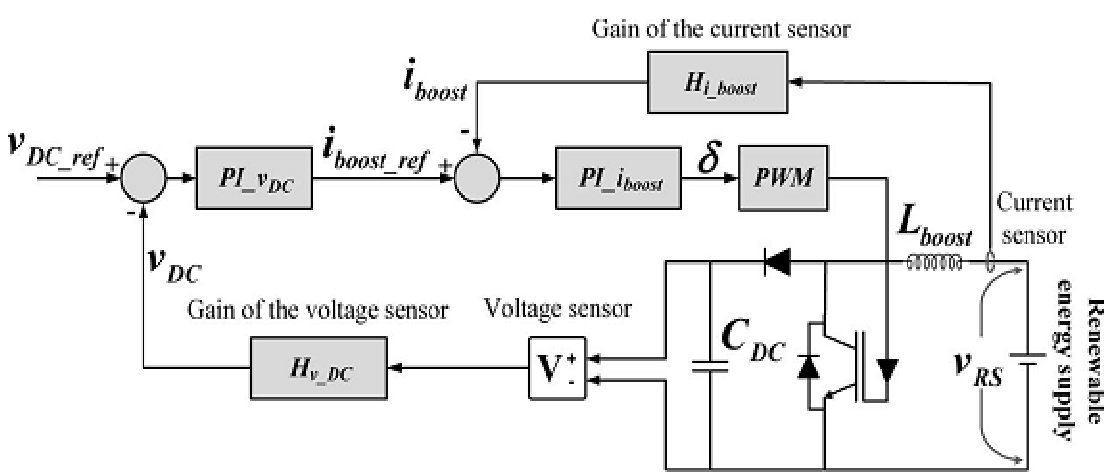

Fig2. Block diagram of the dc voltage/current control

A power plant represents a secondary source (DG systems), while in this study the standard grid is a basic configuration system found in 1547 standard (simulated system) or a California Instruments LX 4500 source (experimental setup). Furthermore, the primary energy used in the proposed DG system is the same as the previously mentioned renewable energy sources.

A dc-dc converter is employed to equalize the dc link voltage and deliver energy for fast transients when required by the local load, while a dc-ac converter is used to guarantee the power quality delivered to customers (local load) and the specific feeder. To avoid disturbances between the dc- ac converter and the feeder, a phase-locked loop (PLL) algorithm [6] associated with the zero voltage crossing detectors was used.

A. DC-DC Converter

A dc-dc step-up converter was used as an interface between the dc source and dc link of the three- phase dc-ac converter, as shown in Fig.2. The step-up converter boosts the dc voltage and supplies the fast transients of energy required for the local load, thereby minimizing disturbances in the feeder current. The behavior of the step-up converter is similar to a voltage source, and the power it delivers to the grid depends on the point of maximum power (PMP) defined by the dc source .

The PMP is obtained using a tracking algorithm, based on the primary energy source. To keep the converters operating in a stable mode, proportional- integral (PI) controllers were used as a control technique to stabilize the L boost current and dc voltage (VDC).

Table I: PI Voltage parameters Of the Dc-Dc converter

$F_{LC}(Hz)$	$mf\,(^{o})$	$V_{DC}(V)$	$L_{boost}(mH)$	$H_{i-boost}$
400	80	1,000	5	1/250

Table II PI Voltage parameters Of The Dc-Dc converter

$F_{LC}(Hz)$	$mf(^{o})$	$V_{DC}(V)$	$C_{DC}(mF)$	H_{V-DC}
50	60	1,000	12	1/1,500

A method based on phase-margin (mf) and cutoff frequency (F_{CL}) was used to obtain the PIs constants (1) and (2), where the open loop gain (G_{OL}), angular frequency (ω_{FCL}), and mf define the PIs constants (k_{prop} and k_{int})

$$k_{prop} \frac{G_{OL}}{F_{CL}} = 1 \quad (1)$$

$$k_{int} = k_{prop} \frac{w_{F_{CL}}}{\tan(mf)} \quad (2)$$

Tables I and II display the main design parameters to namely, H_{i_boost} and H_{v_DC} gains for the dc current and voltage sensors, respectively.

B. DC-AC Converter

Closed-loop controls of the output current and voltage were implemented to guarantee inverter voltage quality. PIs controllers were also used as the control technique, while the design method of these PIs is the same as that used in the dc-dc step-up converter.

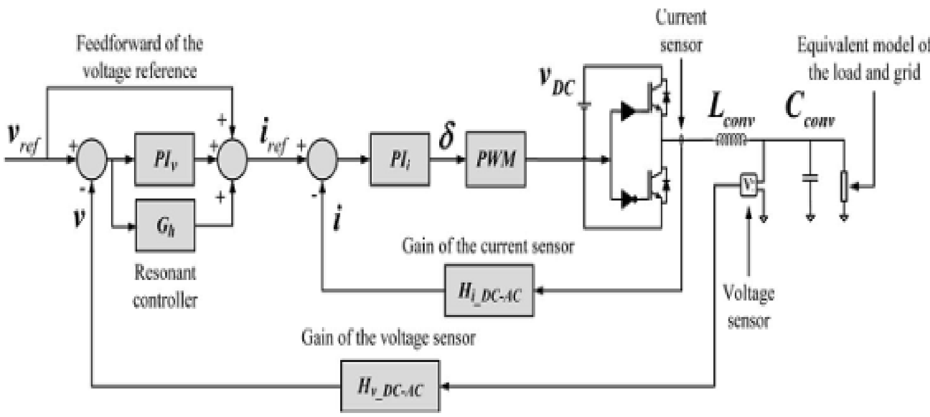

Fig.3 Block diagram of the ac voltage/current control

Table III: Current pi Parameters of the DC-AC Converter

$F_{LC}(Hz)$	$mf\ (^{o}$	$V_{DC}(V)$)	$L_{conv}(mH)$	H_{i_DC-AC}
1,200	70	1,000	2	1/250

Table IV: Voltage pi Parameters Of The DC-AC converter

$F_{LC}(Hz)$	$mf\ (^{o})$	$V_{DC}(V)$	$C_{conv}(\mu F)$	H_{V_DC-AC}
120	70	1,000	15	1/360

Since the closed-loop cutoff frequency of the PI current controller was chosen one decade below the switching frequency, the PI of the current retains a good compensation capability in the frequency range of interest. To improve this capability, a feed forward of the reference voltage could be used to compensate the residual error in the closed-loop gain at low frequencies. Due to its high power and the need for reduced switching frequency, the voltage controller exhibits allow regulation bandwidth (a few hundred Hertz).To improve the control response of the output voltage regulator for fundamental and harmonic components, a resonant controller (3) is placed in parallel along with the convention al voltage PI, thereby reducing the converter impedance.

In equation (3),(h)is the harmonic order, (ω_{ch})is the band pass around the resonance

angular frequency,(ω_0) is the resonance angular frequency, and (k_{ih})is the resonant controller gain[6]. A general block diagram demonstrating the control v is shown in Fig.3.

Tables III and IV present the main design parameters of the ac PIs, where in $H_{i\_DC\_AC}$ and H_{v_DC-AC} are the ac current and voltage sensors gains, respectively

$$G_h = k_{th} \frac{2w_{ch} s}{s^2 + 2w_{ch} s + (hw_0)^2} \quad (3)$$

C. Grid Characteristics

Tables I and II display the main design parameters to determine the PIs constants of the boost converter,

In the simulations, the complete distribution system found in 1547 standard is composed of 13.8-kV feeders connected to a 69-kV radial line through 69/13.8-kV substation transformers, as shown in Fig.1. To insert the DG at the distribution system, a 13.8/0.38 kV distribution network transformer is required to equalize the voltage levels. **See Table: 5**

The line model employed in the simulations took into account the Bergeron's traveling wave method used by the Electromagnetic Transients Program, which utilized wave propagation phenomena and line end reflections. Additionally, a set of switches was inserted between the DGs and distribution system, isolating them from each other to avoid the DG system supplies loads (loads placed in neighboring feeders where the DG was installed) connected to the high voltage side of the distribution transformer.

Due to the high level of power and voltage,

12 kHz was used as the PWM switching frequency for both converters. An experimental setup was built to substantiate the DG operation.

The grid was represented by a California Instruments LX 4500 source and an isolated 220/220-V transformer; the power converter was commanded by an Analog Devices 21992 DSP, while the parameters to design the controllers are those in Tables I– IV, except for the parameters in Table V, which were calculated for a 3-kVA low scale prototype.

To maintain their similarity with the simulations, the switching and sampling frequencies were also kept at 12 kHz. The grid parameters (4) and (5) used in the experimental setup were calculated to have the same dynamic response as the simulated system.

Table V: Modified Parameters of the Converters

$V_{DC}\,(V)$	$C_{DC}\,(\mu F)$	$H_{i-boost}$	H_{V-DC}	H_{i_DC-AC}
330	2,800	1/12	1/360	1/12

The main grid parameters of the equivalent model used in the experimental setup are represented by L_{grid}, R_{grid}, P_{SC}, f, and V^2AB_{source} (inductance and resistance (losses), short-circuit power, rated frequency, and rms voltage (phases A and B), respectively)

$$L_{grid} = \frac{V^2_{AB\,source}}{2\Pi P_{SC} f} \qquad (4)$$

$$R_{grid} \quad (2\Pi f)L_{grid} \quad 1<X<100 \qquad (5)$$

D. Synchronization Algorithm

To connect the DG to the grid, it is essential to synchronize both systems, which is done by means of a PLL algorithm that computes the average of the internal product between v_{source} and the synchronous voltage($v'_\perp$). If this equals zero in steady-state regime, $v'_\perp$ And v_{source} are perpendicular and synchronized.

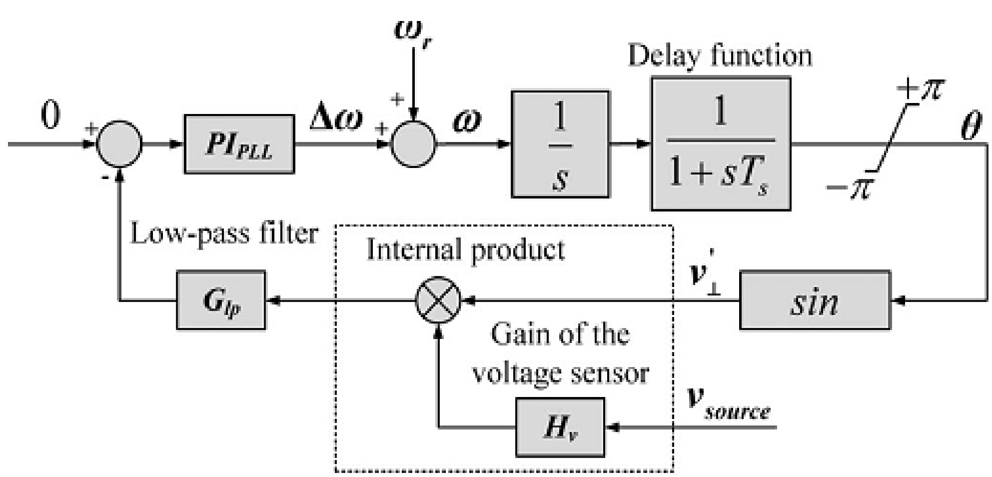

Fig.4: PLL algorithm

$$H_{CL} = \frac{PI_{PLL}}{S} = \frac{k_p s + k_i}{s^2 + k_p s + k_i} \quad (6)$$

To compare the characteristic equation of the prototype transfer function with the PLL closed-loop transfer function (7), PI constants (8) and (9) can be adjusted by choosing the most suitable values for the natural un damped frequency(ω_n) and damping ratio(ξ). To avoid stability problems, ω_n should ideally be greater than one or two periods of the fundamental frequency, and the maximum overshoot lower than 30%.

A general description of the PLL algorithm is found in Fig.4, where ω_r, $\Delta\omega$, and H_v are the rated angular frequency (= 2π60), adjusted angular frequency, and voltage sensor gain (1/360) (voltage measured at the grid), respectively

$$s^2 + k_p s + k_i = s^2 + 2\xi w_n s + w_n^2 \quad (7)$$

Characteristic equation of the PLL transfer function — Characteristic equation of the Prototype transfer function

$$k_p = 2\xi w_n \quad (8)$$

$$k = w^2 \quad (9)$$

III. POWER CONTROL THROUGH THE FEEDER

Energy produced by the renewable energy sources can be transferred to the grid by controlling the amplitude of the voltage produced by the DG, and the angle between the grid voltage and the DG voltage (β angle) through a coupling inductor (L_S). This serves as an additional inductance placed to connect the DG to the grid, or the leakage inductance of the DT. If L_S is a DT parameter, V_{source} must be measured on the high voltage side of the distribution network transformer. To achieve a controlled

To connect the DG to the grid, it is essential to synchronize both systems, which is done by means of a PLL algorithm that computes the average of the internal product between v_{source} and the synchronous voltage(v'⊥). If this equals zero in steady-state regime, v'⊥ And v_{source} are perpendicular and synchronized.

The integration of the angular frequency (ω) then defines the θ angle (θ=wt) used as the argument to Produce v'⊥. Due to the high sampling and switching frequency Ts≈0, the delay block can be dismissed in the PLL closed loop transfer function power flow from the DG to the grid, the DG voltage angle (V_A) must be ahead of the grid voltage angle ($V_{Asource}$). When this occurs, the DG delivers active power to the grid, as shown in Fig.5.

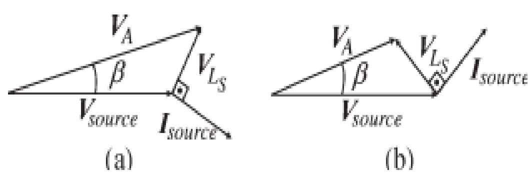

Fig.5: Phasor diagrams. (a) Delivering active and reactive power. (b) Delivering active and absorbing reactive power

The same analysis is can be applied to the ac voltage amplitude produced by the DG: if the amplitude of V_A is greater than $V_{Asource}$ the DG delivers reactive power to the grid; however, if the amplitude of V_A is less than $V_{Asource}$ the DG absorbs reactive power from the grid.

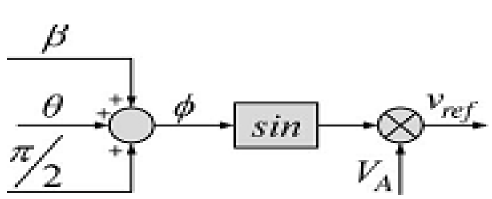

Fig.6 Determination of the voltage reference

The β angle is determined by the average power flowing to the grid (P_{source}), the connection reactance (X_{Ls}), the rms phase voltage ($V_{Asource}$) synthesized by the grid, and the rms voltage produced (V_A) by the DG according to (10). After defining the β angle, the DG voltage amplitude of V_A must be adjusted according to (11), where $V_{Asource}$ and X_{LS} are the same parameters described in (10). If Q_{source}=0 the unity power factor (PF) to the feeder is obtained. Additionally L_S is designed for a small voltage variation on the ac local voltage produced by the dc-ac inverter [7]-[10]. In Fig.6, the voltage reference (V_{ref}) of the dc-ac power converter is determined by displacing θ by π/2 and adding the β angle to the result. The φ angle is then used as the argument of a sinusoidal function and multiplied by V_A to obtain the voltage reference that must be synthesized at the VSI terminals

$$\beta = \sin^{-1}\left(\frac{P_{source} X_{L_s}}{V_{A_{source}} V_A} \right) \quad (10)$$

$$V_A = \sqrt{2} \left(\frac{\ldots_{A_{source}} \ldots_{source} \ldots_{L_s}}{V_{A_{source}} \cos \beta} \right) \quad (11)$$

BLDC MODEL

The BLDC motor is an AC synchronous motor with permanent magnets on the rotor (moving part) and windings on the stator (fix part). Permanent magnets create the rotor flux. The energized stator windings create electromagnet poles. The rotor (equivalent to a bar magnet) is attracted by the energized stator phase, generating a rotation. By using the appropriate sequence to supply the stator phases, a rotating field on the stator is created and maintained. This action of the rotor - chasing after the electromagnet poles on the stator - is the fundamental action used in synchronous permanent magnet motors. The lead between the rotor and the rotating field must be controlled to produce torque. This synchronization implies knowledge of the rotor position. On the stator side, three phase motors are the most common. These offer a good compromise between precise control and the number of power electronic devices required to control the stator currents. For the rotor, a greater number of poles usually create a greater torque for the same level of current. On the other hand, by adding more magnets, a point are reached where, because of the space needed between magnets, the torque no longer increases. The manufacturing cost also increases with the number of poles. As a consequence, the number of poles is a compromise between cost, torque and volume.

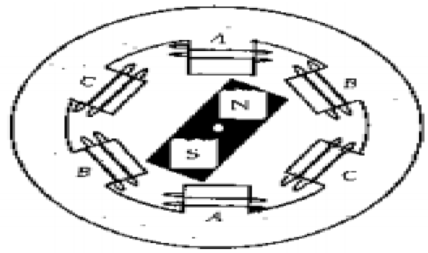

Fig.7: Single Permanent Magnet Pair Pole Rotor

The BLDC Motor Control

The key to effective torque and speed control of a BLDC motor is based on relatively simple torque and Back EMF equations, which are similar to those of the DC motor, The Back EMF magnitude can be written as:

$$E=2NlrB\omega \quad (12)$$

And the torque term as

$$T = \left(\frac{1}{2} i^2 \frac{dL}{d\theta} \right) - \left(\frac{1}{2} B^2 \frac{dR}{d\theta} \right) + \left(\frac{4N}{\pi} Brl\pi i \right) \quad (13)$$

Where N is the number of winding turns per phase, l is the length of the rotor, r is the internal radius of the rotor, B is the rotor magnet flux density, ω is the motor’s angular velocity, i is the phase current, L is the phase inductance, θ is the rotor position, R is the phase resistance.

Matlab/Simulink Results

Here simulation is carried out in several cases, in that 1) Implementation of Proposed Converter Operating of Proposed Converter Operating with Distributed Generation with BLDC Drive System.

Case 1: Implementation of Proposed Converter Operating with Distributed Generation Scheme

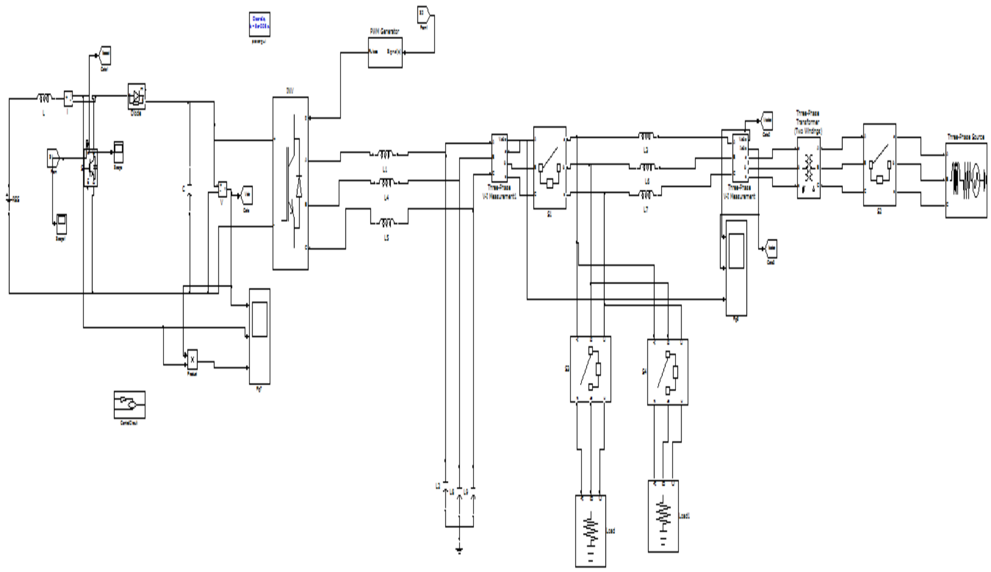

Fig.8 Matlab/Simulink Model of Proposed Converter Operating with Distributed Generation Scheme

Fig.8 shows the Matlab/Simulink Model of Proposed Converter Operating with Distributed Generation Scheme using Matlab/Simulink Software package.

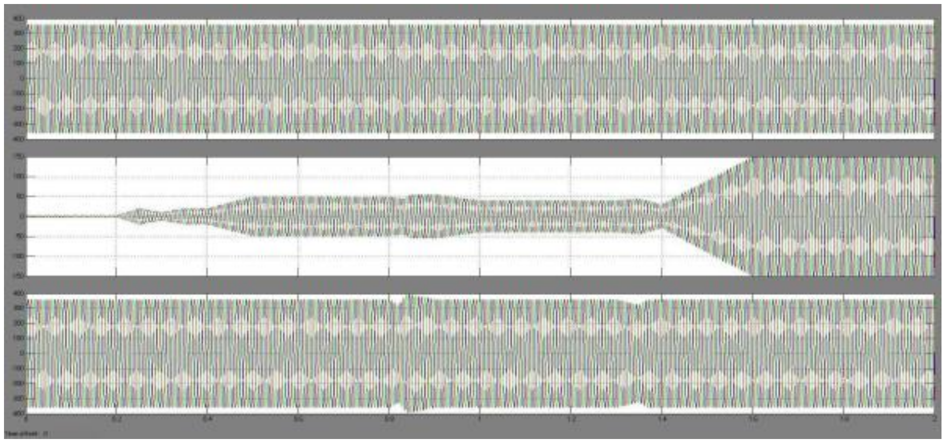

Fig. 9. DG absorbing active power from the grid

Fig. 9. Shows the DG absorbing active power from the grid, subsequently, a soft transfer of power starts at 0.2 s of the simulation range, followed by a base load operation. Due to the method used synchronization and soft transfer of power minimal disturbances are observed in the grid.

Fig. 10 shows the Load currents and voltages produced by the DG with nonlinear load. To observe the system's capability, the minimal value of active and reactive power flows through the grid, with the nonlinear load represented by a non controlled three-phase power rectifier plus RC load that demands around 50 kVA from the DG.

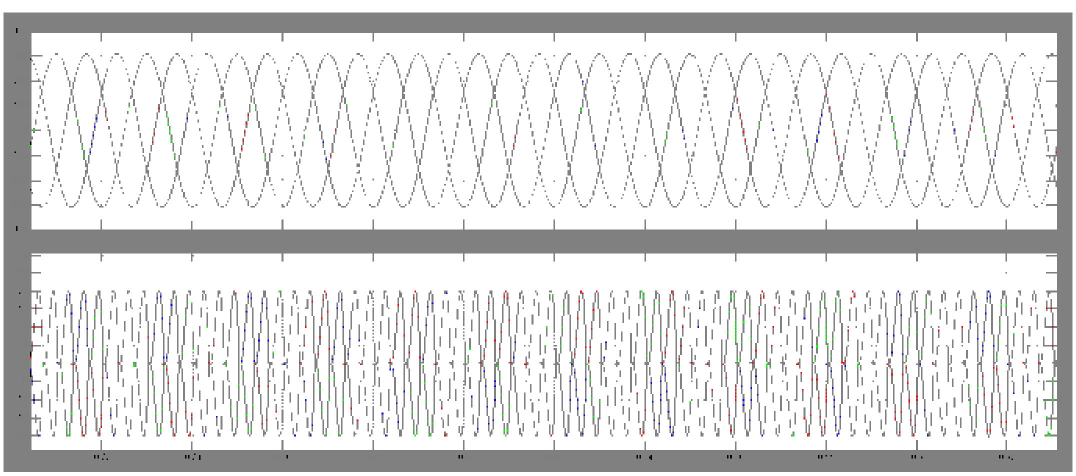

Fig. 10. Load currents and voltages produced by the DG with nonlinear load.

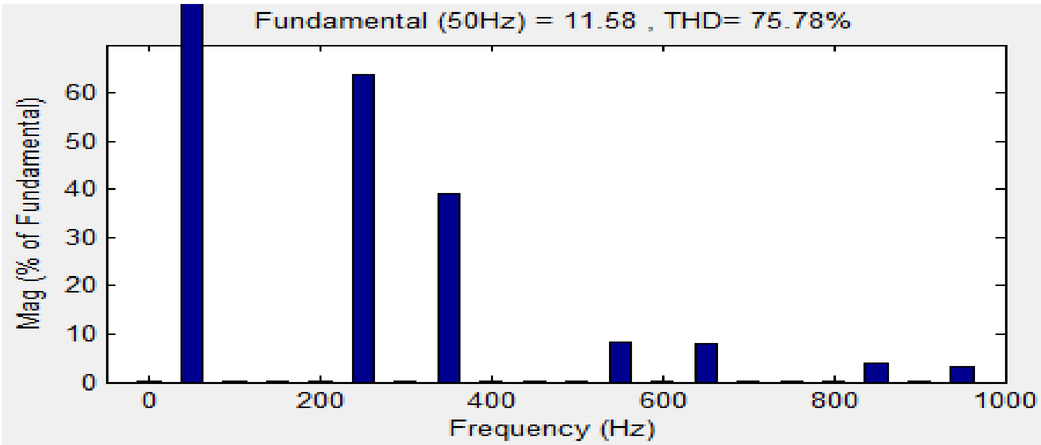

Fig.11 THD analysis of Current

Fig.11 shows the THD analysis of Current, attains 75.78%. The THD of the voltage imposed by the VSI even with the resonant controller compensating the 1st, 3rd, and 5th to 15th harmonics, however, the THD of the load current achieves more than 70%.

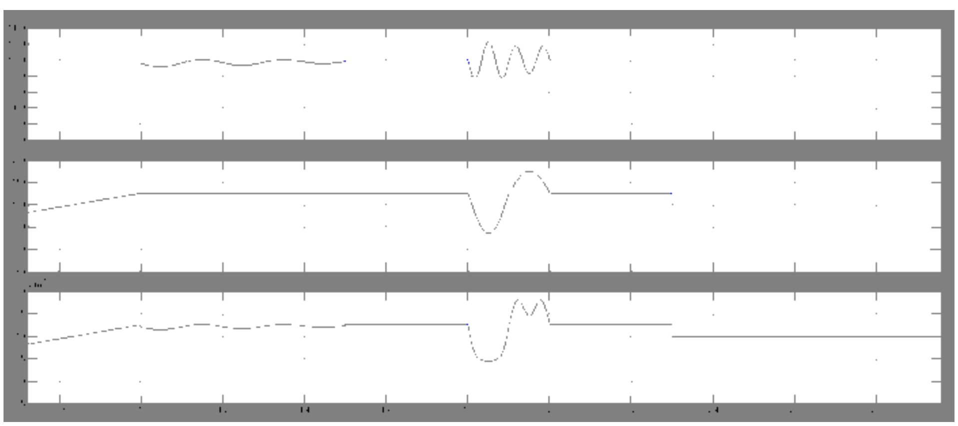

Fig.12 (a) Source Side Voltage, Current, Power

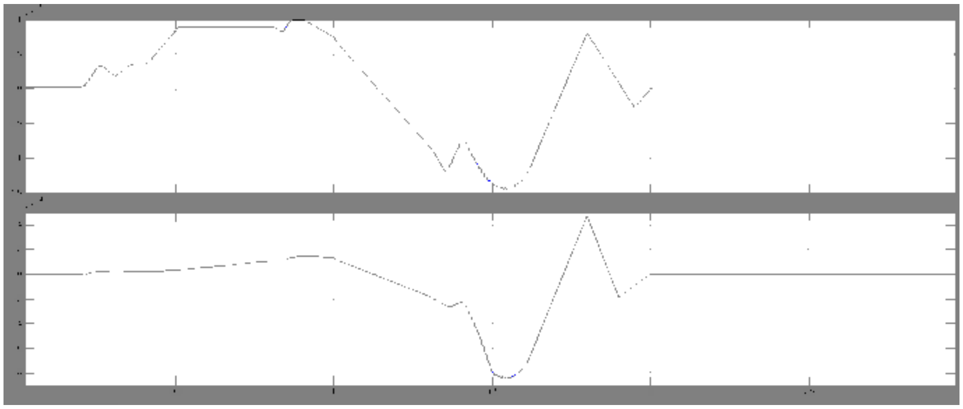

Fig.12 (b) Grid Active & Reactive Power

Fig.12 (a) Source Side Voltage, Current, Power from the DG system and (b) Grid side Active & Reactive Power, islanding with zero power flow condition.

Fig.12 shows the (a) Source Side Voltage, Current, Power from the DG system and (b) Grid side Active & Reactive Power, islanding with zero power flow condition. Identifies the effect of the islanding mode compared with the load connection or power transfer to the grid. In each case, the islanding mode did not affect the dc link voltage and power, or the ac power flow through the grid, which was not the case for the load connection or power transfer.

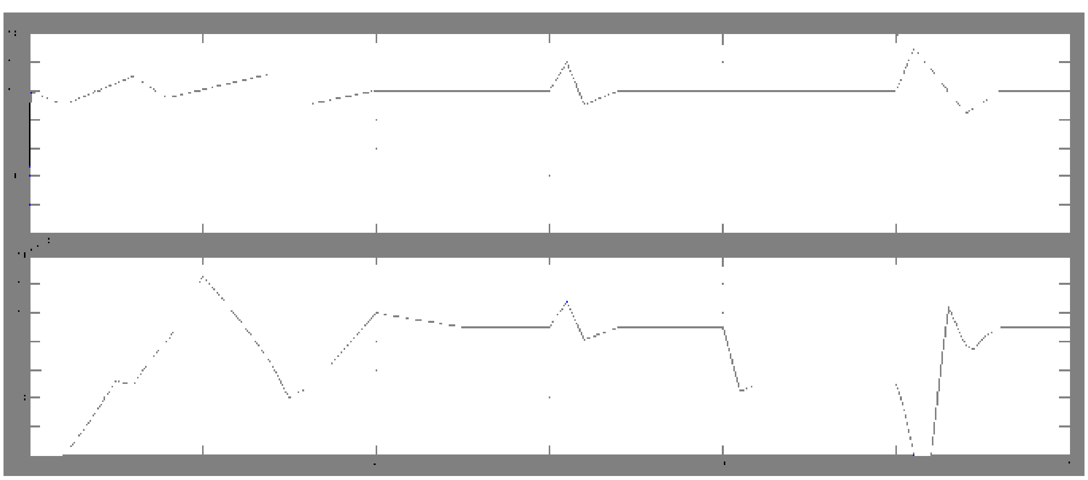

Fig.13 (a) Source Voltage & Power

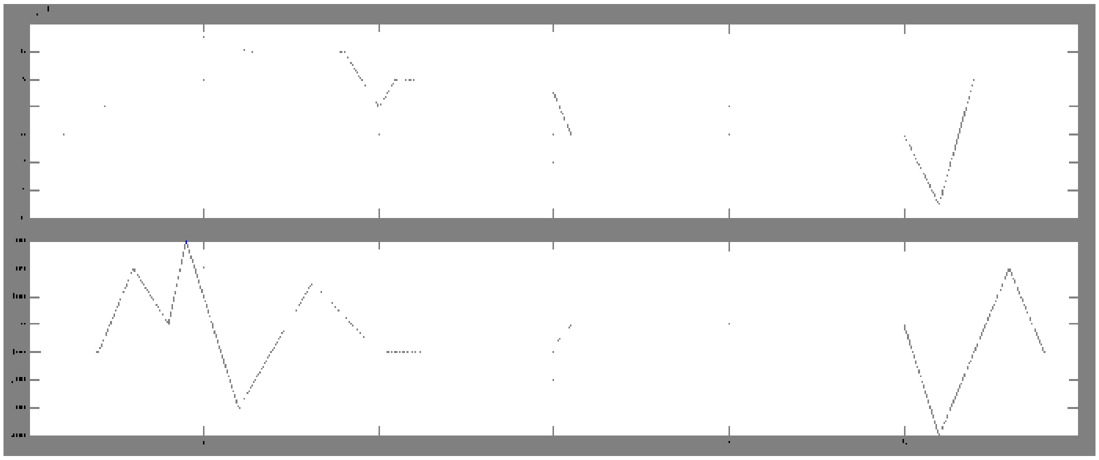

Fig.13 (b) Grid Active & Reactive Power

Fig.13 (a) Source Side Voltage, Power from the DG system and (b) Grid side Active & Reactive Power, another important aspect of the DG operation is the islanding mode followed by a reconnection. As above, the condition performed here considers a limited power level exchanged with the grid.

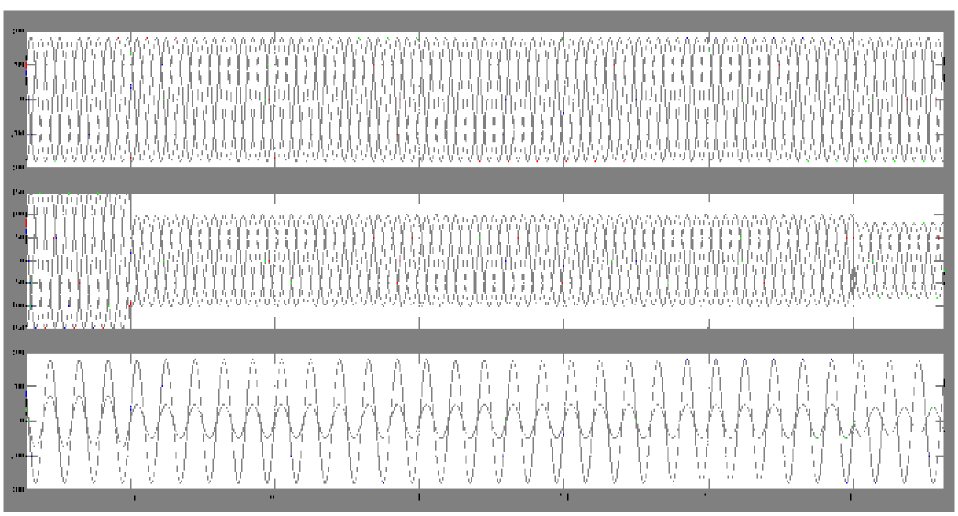

Fig.14 Grid Voltage & Current of the DG system absorbing power from the grid and DG system delivering power to the grid.

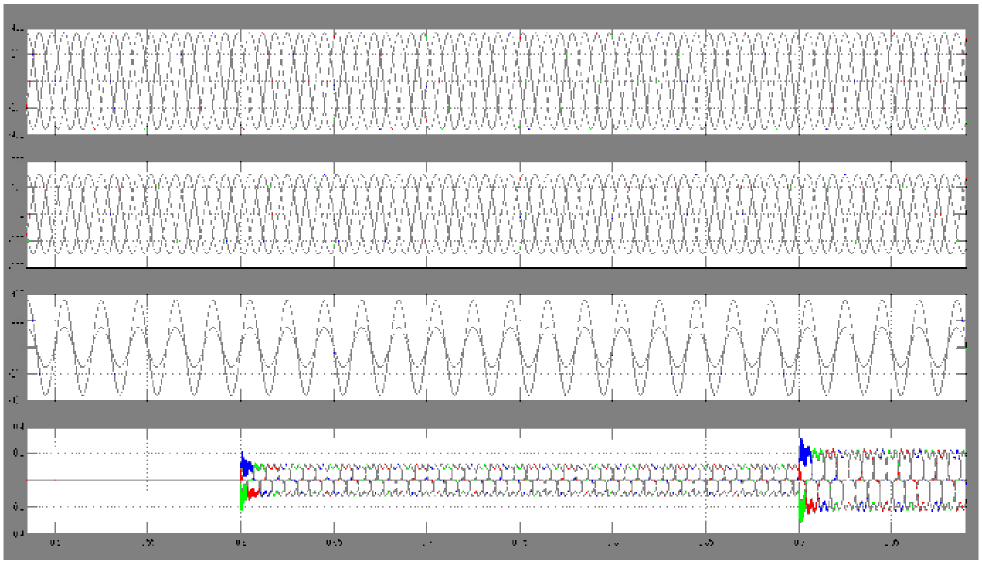

Fig.15 Grid Voltage & Current, Power Factor, Load Current, Nonlinear load connected to the DG terminals and nonlinear load connected to the DG terminals.

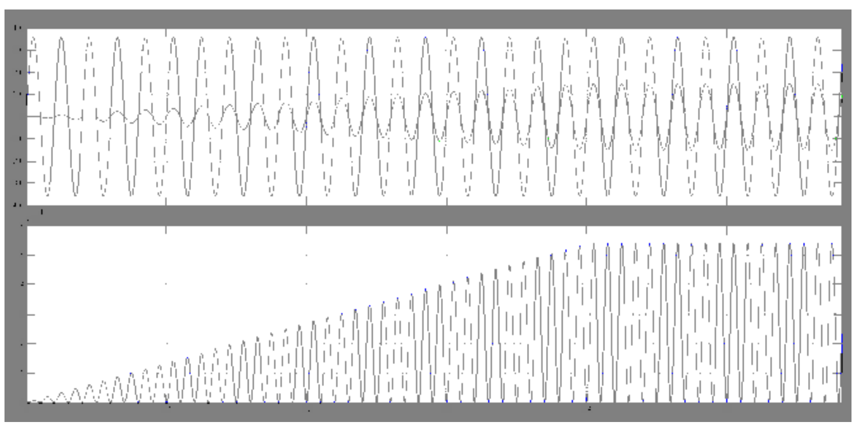

Fig.16 Instantaneous single-phase source power, source voltage, and source current, however, these transients were slowly damped because the amplitude of the DG system is limited, the extra switched resistance placed in parallel with CDC to increase the system damping was not used, and the additional inductance LS was designed to obtain its minimum value.

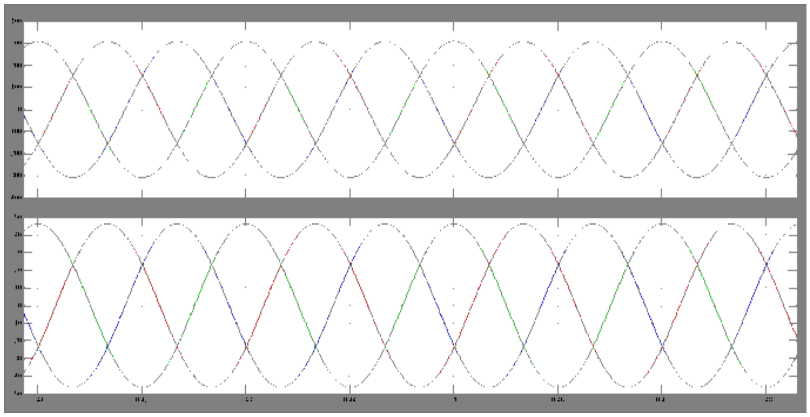

Fig.17 Grid Voltage & Current

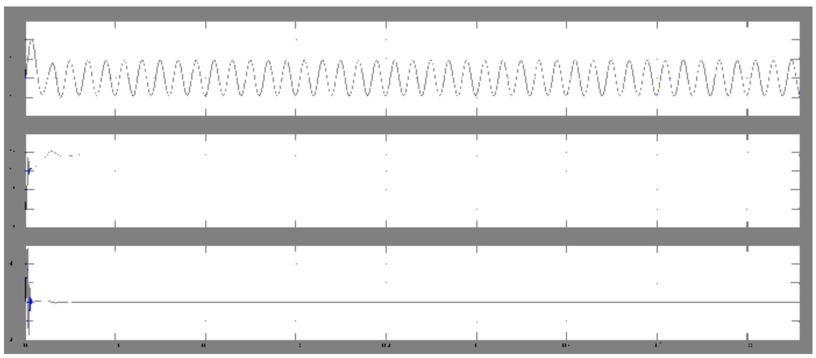

Fig.18 Stator Current, Speed, Electromagnetic Torque

Fig.18 shows the Stator Current, Speed, and Electromagnetic Torque of the Grid connected system with islanding system to update the performance of the drive.

Case 2: Implementation of Proposed Converter Operating with Distributed Generation Scheme with BLDC Drive System.

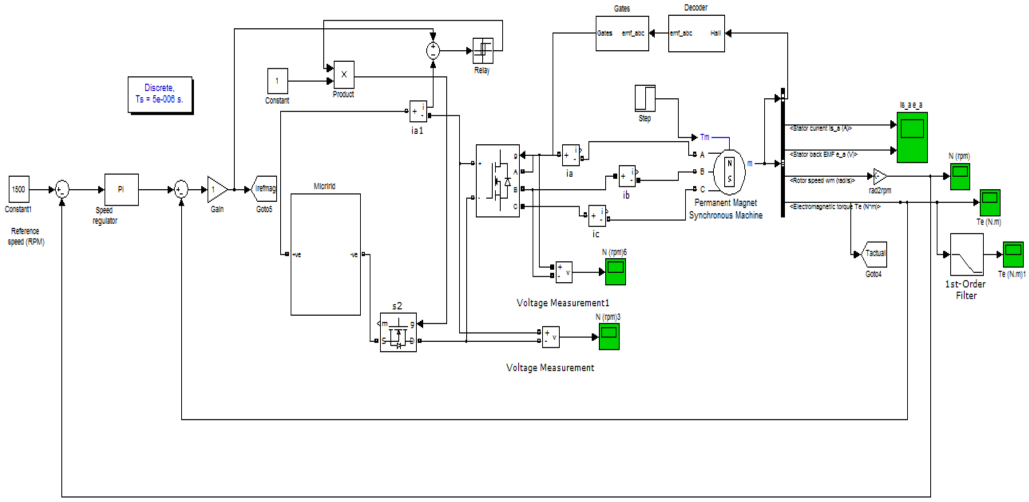

Fig.19: Matlab/Simulink Model of Proposed Converter Operating with Distributed Generation Scheme with BLDC Drive System

Fig.19 shows the Matlab/Simulink Model of Proposed Converter Operating with Distributed Generation Scheme with BLDC drive system using Matlab/Simulink platform.

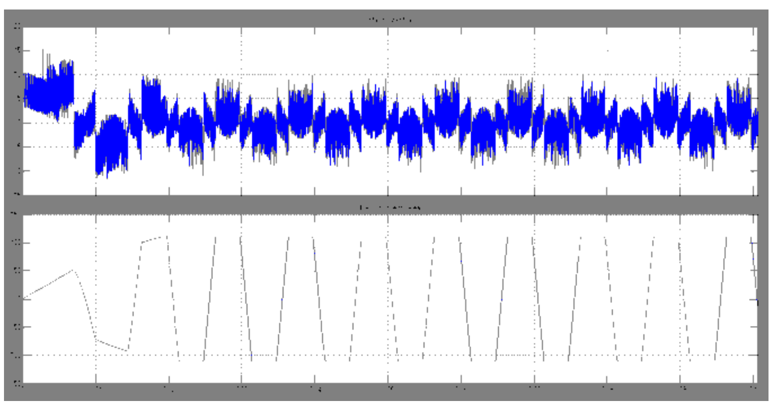

Fig.20 Stator Current and Back EMF

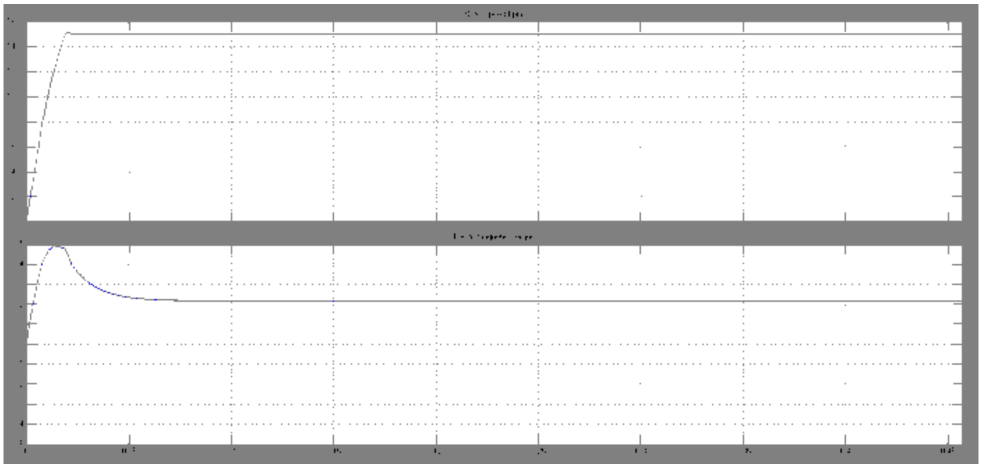

Fig.21: Speed & Electromagnetic Torque

Fig.20 shows the Stator Current and Back EMF of Proposed Converter Operating with Distributed Generation Scheme with BLDC drive system.

Fig.21 shows the Speed & Electromagnetic Torque of Proposed Converter Operating with Distributed Generation Scheme with BLDC drive system.

IV. CONCLUSION

Recent development of high-performance semiconductor power switches such as MOSFETs and insulated-gate bipolar transistors (IGBTs) increases the research interest in high-power converters, such as high step up dc –dc converters. This paper presents an alternative solution to connecting a DG system to the grid/drive application, whereby the amplitude and displacement of the voltage synthesized by the DG is regulated with respect to the grid voltage and the control variable before and after the contingency is always the same. Additionally, a dc-dc step-up converter and a dc-ac VSI are used in a DG system as an interface with the power grid. To improve the DG operation, the dc link voltage must be controlled, in this case by a dc-dc step-up converter. PI controllers associated with resonant regulators were used as a solution to produce distortion-free DG voltage, even when the local load is nonlinear or when distortion occurs in the grid voltage. Although the PLL algorithm tracks as rapidly as possible, the frequency oscillations are slowly damped due to the limits of amplitude. The proposed system is applied to BLDC drive system to update the characteristics of the drive system and simulation results are presented.

REFERENCES

1. Giovani Guarienti Pozzebon, Amilcar Flamarion Querubini Gonçalves, Guido Gómez Peña,Nilton Eufrázio Martinho Moçambique, and Ricardo Quadros Machado. " Operation of a Three-Phase Power Converter Connected to a Distribution System" .IEEE Trans. Ind. Electron., vol., VOL. 60, NO. 5, pp. 1810–1818, MAY 2013.
2. S. Chowdhury, S. P. Chowdhury, G. A. Taylor, and Y. H. Song, "Mathematical modeling and performance evaluation of a stand-alone polycrystalline PV plant with MPPT facility," in Proc. Power Energy Soc. Gen. Meeting—Conversion Delivery Electrical Energy 21st Century, 2008,pp. 1–7.
3. Y. Wen-Chih and H. Wei-Tzer, "A load transfer scheme of radial distribution feeders considering distributed generation," Proc. CIS, pp. 243–248,2010.
4. D. Marquezini, D. B. Ramos, R. Q. Machado, and F. A. Farret,"Interaction between proton exchange membrane fuel cells and power converters for AC integration," IET Renewable Power Generator., vol. 2, no. 3, pp. 151–161, Sep. 2008.
5. S.Chaitusaney and A. Yokoyama, "Impact of protection coordination on sizes of several distributed generation sources," in Proc. IPEC, 2005,pp. 669–674.
6. Blaabjerg, R. Teodorescu, M. Liserre, and A. V. Timbus, "Overview of control and grid synchronization for distributed power generation systems," IEEE Trans. Ind. Electron., vol. 53, no. 4, pp. 1398–14 09,Oct. 2006.
7. J. M. E. Huerta, J. Castello-Moreno, J. R. Fischer, and R. Garcia-Gil, "A synchronous reference frame robust predictive current control for three phase grid-connected inverters," IEEE Trans. Ind. Electron., vol. 57, no. 3,pp. 954– 962, Mar. 2010.
8. P. Rodriguez, A. V. Timbus, R. Teodorescu, M. Liserre, and F. Blaabjerg, "Flexible active power control of distributed power generation systems during grid faults," IEEE Trans. Ind. Electron.,

vol. 54, no. 5, pp. 2583–2592, Oct. 2007.

9. T. Hornik and Z. Qing-Chang, "A current-control strategy for voltage source inverters in micro grids based on H∞ and repetitive control," IEEE Trans. Power Electron., vol. 26, no. 3, pp. 943–952, Mar. 2011
10. J. Balaguer, L. Qin, Y. Shuitao, U. Supatti, and P. F. Zheng, "Control for grid-connected and intentional islanding operations of distributed power generation," IEEE Trans. Ind. Electron., vol. 58, no. 1, pp. 147–157,Jan. 2011
11. R. Q. Machado, S. Buso, and J. A. Pomilio, "A line- interactive single phase to three-phase converter system," IEEE Trans. Power Electron., vol. 21, no. 6, pp. 1628–1636, Nov. 2006.
12. F. Gao, S. Member, and M. R. Iravani, "A control strategy for a distributed generation unit in grid-connected and autonomous modes of operation,"IEEE Trans. Power Del., vol. 23, no. 2, pp. 850–859, Apr. 2008
13. H. Kim, T. Yu, and S. Choi, "Indirect current control algorithm for utility interactive inverters in distributed generation systems," IEEE Trans.Power Electron., vol. 23, no. 3, pp. 1342–1347, May 2008
14. J. M. Guerrero, J. C. Vasquez, J. Matas, L. G. de Vicuna, and M. Castilla, "Hierarchical control of droop-controlled AC and DC micro grids A general approach toward standardization," IEEE Trans. Ind. Electron.,vol. 58, no. 1, pp. 158–172, Jan. 2011.
15. J. M. Guerrero, J. Matas, L. G. de Vicuna, M. Castilla, and J. Miret,"Wireless-control strategy for parallel operation of distributed-generation inverters," IEEE Trans. Ind. Electron., vol. 53, no. 5, pp. 1461–1470, Oct. 2006
16. V. Kaura and V. Blasko, "Operation of a phase locked loop system under distorted utility conditions," IEEE Trans. Ind. Appl., vol. 33, no. 1, pp. 58–63, Jan./Feb. 1997.
17. T. Esram and P. L. Chapman, "Comparison of photovoltaic array maximum power point tracking techniques," IEEE Trans. Energy Convers .,vol. 22, no. 2, pp. 439–449, Jun. 2007
18. S. Buso, S. Fasolo, and P. Mattavelli, "Uninterruptible power supply multi

loop control employing digital predictive voltage and current regulators," IEEE Trans. Ind. Appl., vol. 37, no. 6, pp. 1846–1854,Nov./Dec. 2001.

19. P. Mattavelli, "A closed-loop selective harmonic compensation for active filters," IEEE Trans. Ind. Appl., vol. 37, no. 1, pp. 81–89, Jan./Feb. 2001.
20. C. J. Gajanayake, D. M. Vilathgamuwa, P. C. Loh, R. Teodorescu, and F. Blaabjerg, "Z-source-inverter-based flexible distributed generation system solution for grid power quality improvement," IEEE Trans. Energy Convertor., vol. 24, no. 3, pp. 695–704, Sep. 2009
21. J. Rocabert, G. M. S. Azevedo, A. Luna, J.M. Guerrero, J. I. Candela, andP. Rodríguez, "Intelligent connection agent for three-phase grid-connectedmicrogrids," IEEE Trans. Power Electron., vol. 26, no. 10, pp. 2993–3005,Oct. 2011
22. E. J. Estébanez, V. M. Moreno, A. Pigazo,M. Liserre, and A. Dell'Aquila,"Performance evaluation of active islanding- detection algorithms in distributed-generation photovoltaic systems: Two inverters case," IEEE Trans. Ind. Electron., vol. 58, no. 4, pp. 1185–1193, Apr. 2011.

